energy&fuels

Article

pubs.acs.org/EF

Development of an Electrolytic Cation Exchange Module for the Simultaneous Extraction of Carbon Dioxide and Hydrogen Gas from Natural Seawater

Heather D. Willauer,*[,†] Felice DiMascio,[‡] Dennis R. Hardy,[§] and Frederick W. Williams[∥,⊥]

[†]Materials Science & Technology Division, Naval Research Laboratory, 4555 Overlook Avenue SW, Washington, D.C. 20375, United States

[‡]Office of Naval Research, 875 North Randolph Street, Arlington, Virginia 22203, United States

[§]NOVA Research Inc., 1900 Elkin Street, Alexandria, Virginia 22308, United States

[∥]Chemistry Division, Naval Research Laboratory, 4555 Overlook Avenue SW, Washington, D.C. 20375, United States

ABSTRACT: An electrolytic cation exchange process has been developed to extract large quantities of carbon dioxide (CO_2) from natural seawater where it is in the form of bicarbonate and carbonate, and to simultaneously produce H_2 gas in quantities and ratios (3:1 H_2 to CO_2) intended for future synthesis of hydrocarbons. During the early stages of development, optimizing the energy efficiency and CO_2 production efficiency of the process is key to its future practical implementation. Both efficiencies are impacted specifically by the amount of time needed to re-establish equilibrium conditions in the module after a polarity reversal. Three electrolytic cation exchange module (E-CEM) configurations were tested and evaluated to determine the parameters that had the most significant effects on shortening the re-equilibration times after polarity reversal. From these evaluations, a new fourth custom E-CEM was designed, built, and tested that lowered seawater pH 65% faster so that carbonate and bicarbonate in the seawater were re-equilibrated to CO_2 gas for recovery and the electrical resistance was reduced by 31%. These results are important for the future scale-up and implementation of such a process.

INTRODUCTION

Solutions to solving global increases in anthropogenic levels of CO_2 in the earth's atmosphere have led to extensive research in the development of carbon capture and storage (CCS) technologies.[1−4] The long-term effects of storage in geological formations and in the ocean remain unknown, and as a result there is increasing interest in capturing and recycling CO_2 as a feedstock for the production of energy-rich compounds.[2,3]

CO_2 fixation in microalgae and its conversion to chemicals and polymers will help to reduce atmospheric CO_2 emissions and generate revenue to offset the cost of capture and separation technologies.[2,3] However, these processes require the CO_2 to be extremely pure.[2,3] CO_2 from flue and stack gases contains SO_x that greatly restricts microalgae growth and stops it all together at 50 ppm.[3] In addition, these impurities will rapidly poison catalysts used in the chemical conversion and reduction of CO_2.[1,2] Thermochemical approaches to produce chemicals and fuels from CO_2 (methanol and olefins) require a source of hydrogen.[2,3,5] Since CO_2 purity and the need for hydrogen are relevant to many chemical conversions of CO_2 to chemicals and fuels, new more general approaches to the removal of large amounts of anthropogenic CO_2 from the environment are needed.

The world's oceans contain approximately 100 mg·L^{-1} total carbon dioxide, $[CO_2]_T$, of which 2−3% is dissolved CO_2 gas in the form of carbonic acid, 1% is carbonate, and the remaining 96−97% is bound as bicarbonate.[6,7] Comparing the seawater concentration on a weight per volume basis (w/v) to that of a stack gas (about 300 mg·L^{-1}) and air (about 0.77 mg·L^{-1})[1] strongly suggests the world's oceans could be a key to developing more general and practical approaches to removing and temporarily storing the anthropogenic gas from the environment.

Electrochemical approaches based on continuous electrodeionization (CEDI) principles are being developed to use pH to exploit seawater as a means to recover CO_2 from the sea.[8−11] Johnson et al. demonstrated that when the pH of seawater is decreased to 6 or less, carbonate and bicarbonate in the seawater are re-equilibrated to CO_2 gas (eq 1).

$$HCO_3^- + H^+ \rightleftarrows H_2CO_3 \rightleftarrows H_2O + CO_2(g)\uparrow \quad (1)$$

This method has been the basis for standard quantitative ocean total CO_2 measurements for over 25 years.[12]

In addition to recovery of CO_2 from seawater, the approach described here simultaneously produces hydrogen gas through electrolytic dissociation of water in the cathode compartment. While these electrochemical technologies look promising, they are still in the early stages of development and many challenges remain in scaling and configuring these processes for practical and more energy efficient implementation.[8−11] This work describes the step by step evolution of the electrolytic cation exchange module (E-CEM) developed by the Naval Research Laboratory (NRL). The first three module configurations are based on NRL modifications to commercially available electrodeionization cells. Each of the three different module configurations were designed, tested, and evaluated by

Received: October 6, 2016
Revised: January 4, 2017
Published: January 8, 2017

ACS Publications © 2017 American Chemical Society

DOI: 10.1021/acs.energyfuels.6b02586
Energy Fuels 2017, 31, 1723−1730

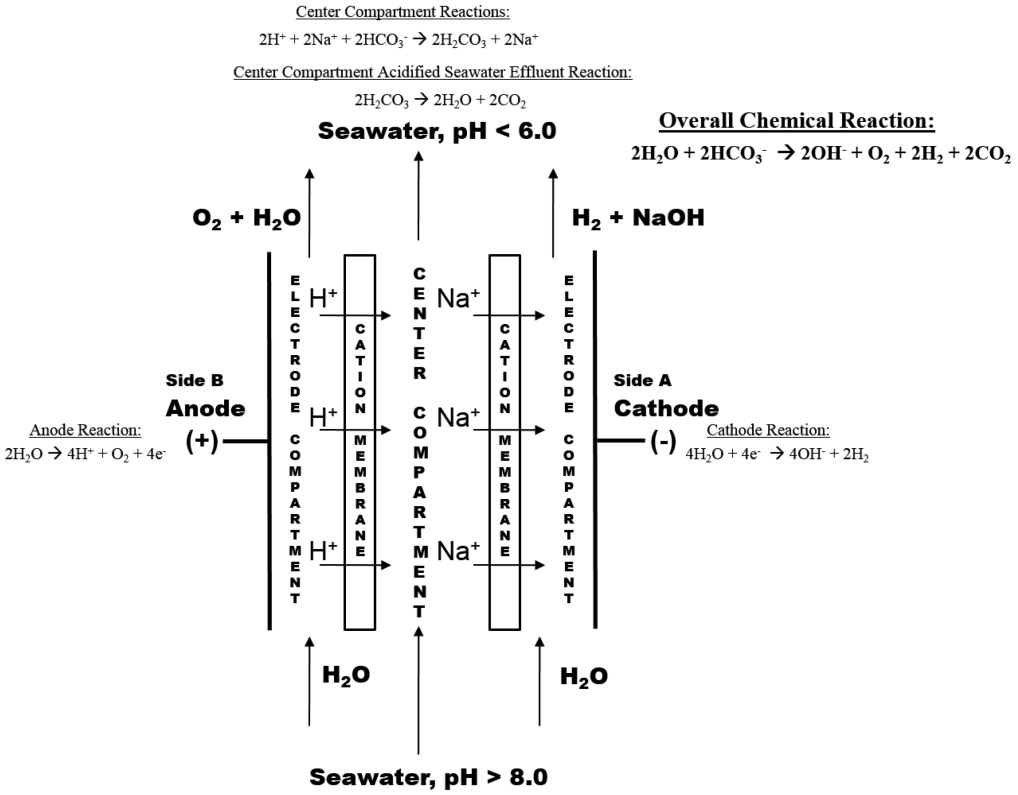

Figure 1. General schematic of the E-CEM configuration.

Table 1. E-CEM Configurations and Component Dimensions

E-CEM Component	E-CEM 1	E-CEM 2		E-CEM 3
	Conf. 1	Conf. 2	Conf. 3	Conf. 4
Center Compartment Width, cm	14.0	14.0		14.0
Center Compartment Height, cm	35.5	35.5		35.5
Center Compartment Thickness, cm	0.90	0.90		0.90
Center Compartment Volume, cm^3	447	447		447
Membrane Active Area, cm^2	497	497		497
Ion Exchange Resin	2.1 eq/L	50% at 2 eq/L	100% at 1 eq/L	none
Electrode Compartment Width, cm	14.0	14.0		14.0
Electrode Compartment Height, cm	35.5	35.5		35.5
Electrode Compartment Thickness, cm	0.45	0.45		0.05
Electrode Compartment Volume, cm^3	224	224		14.4
Membrane Thickness	0.07	0.07		0.07
Electrode Active Area cm^2 (A eq. 15)	497	497		497
Distance Between Electrodes, cm (x eq. 14)	1.94	1.94		1.14
Endplate Material	aluminum	aluminum		PVC
Average Power Consumed, watts	387	540	581	265

measuring the effluent seawater pH, current, voltage, polarity reversal, and electrical resistance profiles as a function of time. These parameters are used to determine and compare how efficient the ionic transport properties in the seawater have been manipulated and improved to re-equilibrate carbonate and bicarbonate in the seawater to CO_2 gas and simultaneously produce hydrogen (H_2) gas in each of the three module configurations. The fourth module configuration was custom designed and built based on the performance evaluations of the first three modified configurations. The objective of the fourth module configuration was to realize a significant improvement in the energy efficiency of lowering seawater pH below 6 in the

DOI: 10.1021/acs.energyfuels.6b02586
Energy Fuels 2017, 31, 1723−1730

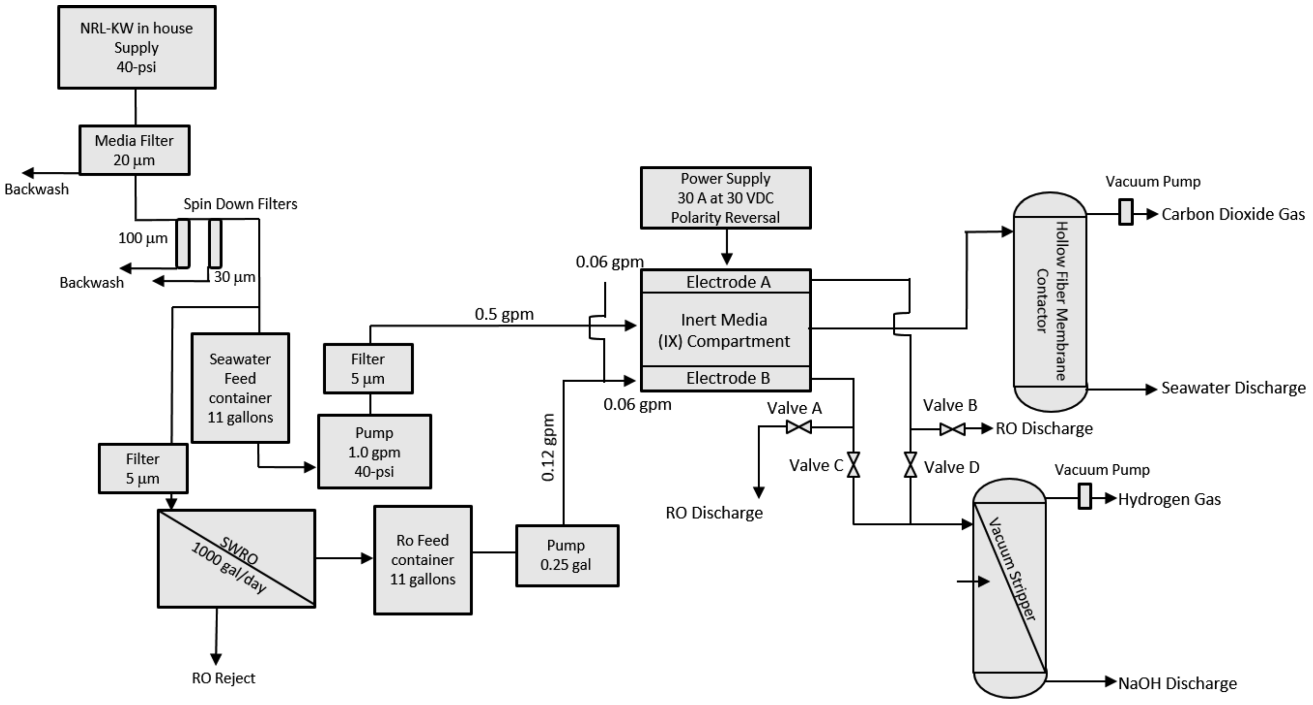

Figure 2. Process flow diagram of the carbon capture process.

E-CEM process. Later development will include maximizing energy efficiencies for H_2 production equivalent to current commercial devices.[13] These data provide insights into how to improve the E-CEM design and efficiencies for future commercial scale applications.

EXPERIMENTAL METHODOLOGY

Electrolytic Cation Exchange Module. Figure 1 shows a schematic that describes the general E-CEM configuration, and Table 1 provides the dimensions and electrical specifications of each of the four configurations. The E-CEMs all include a center compartment, electrode compartments (cathode and anode capable of reversing polarities), and two cation-permeable membranes which separate the three compartments. Extruded cation-permeable heterogeneous monolithic polyethylene membranes incorporate gel polystyrene cross-linked with divinylbenzene and functionalized with sulfonic acid groups. The acid functionality provides discrete channels for cations to migrate through the polymer matrix while blocking the passage of anions. These membranes are from Ionpure (Lowell, MA, USA) and have the following properties: permselectivity greater than 89% at 0.1/0.05 M KCl, maximum current density of 825 $A{\cdot}m^{-2}$, ion-exchange capacity greater than 2 $mequiv{\cdot}g^{-1}$, electrical resistance of less than 30 $\Omega{\cdot}cm^2$ at 50 ppm of NaCl, water permeability at 5 psi of less than 3 $mL{\cdot}h^{-1}{\cdot}ft^{-2}$, and they are chemically stable between pH 0.5 and pH 13.5 up to 90 °C.

Figure 1 shows the electrode compartments of the module defined as side B and side A for each of the four module configurations. Polarity A and polarity B designate the electrode compartment (side A or side B) that is functioning as the anode during the polarity cycle (modules pictured operating as polarity B, Figure 1).

The first three E-CEM configurations were constructed from standard commercially available electrodeionization cells (Ionpure LX-X Module). The end plates of these three modules were composed of aluminum and contained separate electrode compartments made from polyethylene. The flat and solid anode and cathode titanium electrodes in the compartments were coated with platinum and had an electrode active area of 497 cm^2 (Table 1). Inert plastic particles were used in the center compartment of these configurations to serve as a support structure for the membranes, and the electrode compartments contain cation-exchange resin. In the first E-CEM configuration 100% strong cation-exchange resin from Rohm & Haas (IR-120) was used in both electrode compartments, and its capacity was 2.1 $equiv{\cdot}L^{-1}$.

The second and third configurations of the E-CEM were tested simultaneously in the same module. Each electrode compartment was configured to contain 50% less ion-exchange capacity. However, each electrode compartment in the same module used different ion-exchange resin to achieve this objective. Side B contains 100% strong acid ion-exchange resin with a capacity of 1 $equiv{\cdot}L^{-1}$. Side A contains 50% less of the strong acid cation-exchange resin that was used in the original module (2.1 $equiv{\cdot}L^{-1}$). This resin is uniformly mixed with 50% inert material to fill the compartment.

The fourth E-CEM configuration was custom designed and built without ion-exchange resin in the electrode compartments and inert material in the center compartment. The end plates of the module were combined with the electrode compartment and constructed from poly(vinyl chloride) (PVC). Titanium mesh electrodes coated in platinum in the compartments were used as the cathode and anode. The electrode active area was 497 cm^2. Table 1 shows that the electrode thickness and volume along with the distance between the electrodes in this configuration have been greatly reduced to maintain ion transport and electrical efficiencies.

The resins and membranes used in the modules are typically used for years in commercial water treatment electrolysis processes. The water filtration and current densities are well within the specifications of all products used to construct the module. After 4 years of intermittent use, no degradation or deterioration of the resin or membranes used to construct the modules has been observed.[10]

Carbon Capture Skid and Procedure. Since natural Key West seawater was used, the work was performed at the Naval Research Laboratory's Corrosion Laboratory located at Key West, FL, USA to evaluate the E-CEM's performance. The module was incorporated into a portable skid along with a reverse osmosis (RO) unit, power supply, pumps, a membrane contactor CO_2 gas recovery system, hydrogen gas vacuum tower, and gas analyzer to form a carbon and hydrogen capture system, all operated by a control logic capable of maintaining automatic operation safely on a continual basis. Figure 2 is a process flow diagram of the carbon capture skid. Seawater was supplied to the skid by an in-house 40 psi supply line. The water was filtered by two spin-down filters in series (100 and 30 μm). After filtration, a portion of the seawater was sent to an 11 gallon high density polyethylene

DOI: 10.1021/acs.energyfuels.6b02586
Energy Fuels 2017, 31, 1723−1730

container that functions as the seawater feed container. Before the seawater in the seawater feed tank was fed to the center compartment of the E-CEM at 0.5 gallon·min^{-1} (1900 mL·min^{-1}), it was pumped through a 5 μm filter cartridge. The other portion of the seawater supply was fed through a 5 μm filter cartridge to the RO system for processing. The RO system was an EPRO-1000SW from Crane Environmental, Inc. (Venice, FL, USA) that is capable of producing 0.7 gallons·min^{-1} (1000 gallons·day^{-1}) of permeate (fresh water quality from seawater at a conductivity of approximately 200 μS·cm^{-1}). This water was stored in an 11 gallon polyethylene container that is specified as the RO feed container. This water was the feedwater to the electrode compartments of the E-CEM at a total flow rate of 0.12 gallon·min^{-1} (460 mL·min^{-1}). The flow was split within the E-CEM resulting in electrode compartment flow rates of 0.06 gallon·min^{-1} (230 mL·min^{-1}) to each electrode compartment.

A Mastech HY3030EX 0−30 A, 0−30 V, regulated DC power supply was used to supply the current to the E-CEM electrodes. The seawater pH changed as a function of applied current to the E-CEM. Effluent seawater pH was monitored continuously using a standard combination electrode as it exited the center compartment of the module. Vision 290 Unitronics hardware and software were used to control the system components (RO, E-CEM, well pump, vacuum towers, vacuum pumps, solenoid valves, and power supply) so they operated and functioned together as an integrated unit on a continual automated basis, with limited operator control required. The CO_2 gas from the effluent acidified seawater flowing at 0.5 gallons·min^{-1} was vacuum stripped using a commercial membrane contactor (Liqui-Cel 2.5 in. × 8 in. polyethylene hollow fiber membrane contactor (Membrana-Charlotte)). The $[CO_2]_T$ content of the acidified effluent seawater was measured by coulometry (UIC Inc., Joliet, IL, USA) after contact with the membrane contactor to determine the efficiency of the extraction method.[12] The $[CO_2]_T$ content of the natural Key West seawater before acidification was measured to be approximately 100 mg·L^{-1}. Simultaneously, a standard purpose-built hydrogen gas vacuum tower processed the water from the acting cathode compartment of the module as it liberated H_2 gas. The H_2 gas was measured qualitatively throughout the operation by a standard Honeywell gas analyzer (7866 digital gas analyzer), as was the CO_2.

RESULTS AND DISCUSSION

The E-CEM depicted in Figure 1 is configured as a three compartment module (anode compartment, central seawater compartment, and cathode compartment). The E-CEM takes advantage of continuous electrodeionization (CEDI) principles of removing ionizable species from liquids by manipulating their ionic transport properties using an applied electrical potential, ion-exchange resins where used, and semipermeable ion-exchange membranes as electrically active media.[14−19]

In the continuous flow process shown in Figure 2, seawater is passed through the center compartment of the E-CEM (Figure 1) at a flow rate of 0.5 gal·min^{-1} (1900 mL·min^{-1}), while RO water is passed through the anode and cathode compartments each at 0.06 gal·min^{-1} (230 mL·min^{-1}). The principle chemical reactions within the E-CEM are simplified as shown in eqs 2−6. When direct current is applied to the module, H^+ ions and O_2 gas are generated at the anode by the oxidation of the anolyte RO water (eq 2).

at the anode:

$$2H_2O \rightarrow 4H^+ + O_2 + 4e^- \quad (2)$$

The O_2 gas is flushed from the anode compartment with the flow of the anolyte (deionized water). The H^+ ions are driven from the surface of the anode, through the cation-permeable membrane, and into the center compartment where they replace the Na^+ in the flowing seawater. This causes the effluent seawater to be acidified without the need for any additional chemicals. At a seawater pH less than or equal to 6, the bicarbonate and carbonate in the seawater are re-equilibrated to carbonic acid (eq 3).

center compartment:

$$2H^+ + 2Na^+ + 2HCO_3^- \rightarrow 2H_2CO_3 + 2Na^+ \quad (3)$$

The CO_2 from the carbonic acid in the effluent acidified seawater is vacuum stripped by a gas-permeable membrane contactor (eq 4).

center compartment acidified seawater effluent:

$$2H_2CO_3 \rightarrow 2H_2O + 2CO_2 \quad (4)$$

The Na^+ ions from the seawater in the center compartment are passed through the cation-permeable membrane closest to the cathode. Water is decomposed at the cathode to H_2 gas and OH^- (eq 5).

at the cathode:

$$4H_2O + 4e^- \rightarrow 4OH^- + 2H_2 \quad (5)$$

The Na^+ reacts with the OH^- to effectively produce sodium hydroxide in the cathode compartment. The NaOH and H_2 gases are continuously flushed from the cathode compartment with the flow of the catholyte (RO water). The acidified seawater is recombined with the solutions from the cathode and anode compartments. The overall reaction in eq 6 shows that chemically each mole of HCO_3^- in seawater is replaced with a mole of OH^-.

overall chemical reaction:

$$2H_2O + 2HCO_3^- \rightarrow 2OH^- + O_2 + 2H_2 + 2CO_2 \quad (6)$$

The amount of H^+ generated by the anode is proportional to the applied electrical current, which follows Faraday's law. The anode and cathode reactions used to theoretically determine the amount of H^+, OH^-, H_2, and O_2 produced per amp·second of current passed through the electrodes are provided in eqs 7−12 as follows:

anode reaction:

$$\left(\frac{(1/4)\ \text{mol of } O_2}{96487\ \text{A·s}}\right)\left(\frac{60\ \text{s}}{\text{min}}\right) = 0.000155\ \frac{\text{mol of } O_2}{\text{A·min}} \quad (7)$$

$$\left(\frac{1\ \text{mol of } H^+}{96487\ \text{A·s}}\right)\left(\frac{60\ \text{s}}{\text{min}}\right) = 0.000622\ \frac{\text{mol of } H^+}{\text{A·min}} \quad (8)$$

cathode reaction:

$$\left(\frac{(1/2)\ \text{mol of } H_2}{96487\ \text{A·s}}\right)\left(\frac{60\ \text{s}}{\text{min}}\right) = 0.000311\ \frac{\text{mol of } H_2}{\text{A·min}} \quad (9)$$

$$\left(\frac{1\ \text{mol of } OH^-}{96487\ \text{A·s}}\right)\left(\frac{60\ \text{s}}{\text{min}}\right) = 0.000622\ \frac{\text{mol of } OH^-}{\text{A·min}} \quad (10)$$

Therefore, seawater with a HCO_3^- concentration of 142 ppm (0.0023 M) and a flow rate of 1900 mL·minute^{-1} will require a theoretical applied minimum current of 7.0 A to lower the pH to less than 6.0 and convert HCO_3^- to H_2CO_3 (eq 11).

$$\frac{\left(\frac{0.0023\ \text{mol of } HCO_3^-}{\text{L}}\right)\left(\frac{1.89\ \text{L}}{\text{min}}\right)}{\left(\frac{0.000622\ \text{mol of } H^+}{\text{A·min}}\right)} = 7.0\ \text{A} \quad (11)$$

DOI: 10.1021/acs.energyfuels.6b02586
Energy Fuels 2017, 31, 1723−1730

The theoretical amount of CO_2 that can be removed from the acidified seawater is 0.0023 mol·L^{-1}. The theoretical amount of H_2 gas generated at 7.0 A is

$$\left(\frac{(1/2)\ \text{mol of H}_2}{96487\ \text{A·s}}\right)\left(\frac{60\ \text{s}}{\text{min}}\right)(7.0\ \text{A}) = 0.0022\ \frac{\text{mol of H}_2}{\text{min}} \quad (12)$$

Increasing the current increases the molar ratio of the measured hydrogen to CO_2 with no effect on the operation of the E-CEM. H^+ generated will either exchange with Na^+ in the seawater to further lower its pH or migrate through the center compartment and into the cathode compartment where it will combine with OH^- to form water. The ability to control the molar ratio of H_2 produced at the cathode for thermal catalytic processes to make hydrocarbons from CO_2 is a unique feature of this process. Close examination of eqs 2, 3, and 5 reveal the following: (1) every unit (mole) of electricity consumed makes a 1/2 mol of H_2 at the cathode in eq 5; (2) simultaneously for every mole of electricity consumed, a 1/4 of a mole of O_2 is produced at the anode in eq 2; (3) simultaneously for every mole of electricity consumed, a mole of H^+ is produced in the anode compartment in eq 2; and (4) finally for every mole of H^+ produced in the anode compartment, 1/2 of a mole is used to acidify seawater below pH 6 in the central compartment in eq 3 resulting in the recovery of CO_2. Therefore, the overall E-CEM process makes the electrical energy needs for CO_2 production from seawater an energetically free byproduct of the hydrogen and oxygen gas production. The operational current during these tests (20 A) theoretically produced 3 times more H_2 gas (0.006 mol of H_2·min^{-1}) than that shown in eq 12.

The E-CEM is tested and evaluated in four different configurations. The first three configurations utilize commercially available electrodeionization cells that contain active media (ion-exchange material) in the electrode compartments. The use of commercially available electrodeionization cells provides a cost-effective approach to characterize the process (seawater flow rate and applied current) and to determine the design parameters needed to build a custom module.

The ion-exchange material in the first three configurations serves two purposes. First, it is an immobile electrolyte that promotes conductivity and ion transport within the module since freshwater permeate (RO permeate) is used in the electrodes. Second it provides turbulent flow for uniform gas removal (H_2 and O_2). This is critical as it provides uniform current distribution. As the development of the E-CEM evolves from initial proof of concept and feasibility to a custom designed module, the active media (ion-exchange material) in the electrode compartments is systematically changed and ultimately removed. The distance between electrodes is shortened, and the flow channels are provided on the back side of the electrodes for effective gas removal (electrode form is changed from planar to mesh). The flow channels allow the electrode flow velocity to be totally independent of gas removal, allowing lower electrode flow rates to be evaluated, thus lowering the required amount of fresh water. The uniform current distribution across the modules was not changed. While these changes have been designed to have little effect on the overall chemistry within the module (eqs 2−12), they do significantly impact the transport properties of the ions. These transport properties affect how fast the chemistry inside the module occurs and how efficient the module can re-establish equilibrium conditions when the polarity of the module is switched.

Polarity switching is a common practice in the electrodialysis reversal (EDR) process to desalinate brackish ground and surface waters, and it is designed into the system to provide electrode regeneration at regular intervals called polarity cycles.[14] During a polarity cycle the current begins to decrease over time. This is measured by an increase in electrical resistance over time. This increase is most likely from mineral deposition occurring on the electrode surface of the cathode in high pH solutions (pH < 12). Polarity cycling is designed to minimize the reduction in current efficiencies and prevent potential pressure drops caused by the mineral deposition on the electrode surface. This feature could be critical to the long-term stability, operation, and future application of the technology. It takes 45 min at an applied module current of 20 A for the current to decrease as the electrical resistance begins to increase in the first three module configurations. After 45 min the polarity is switched and the cathode is regenerated. A 45 min time interval defines the length of a polarity cycle in these studies.

Figure 3 compares the pH profiles as a function of time for four different E-CEM configurations at an applied module current of 20 A. In the first configuration, 100% strong cation-exchange resin having a capacity of 2.1 equiv·L^{-1} is used in both electrode compartments. Polarity A and polarity B designate the electrode compartment (side A or side B, Figure 1) that is functioning as the anode during the polarity cycle (module in Figure 1 pictured operating as polarity B). A flush cycle is used to wash the excess H_2, NaOH, O_2, and H^+ from the electrode compartments before the polarity was actually switched. Figure 3 shows this module configuration took approximately 27 min

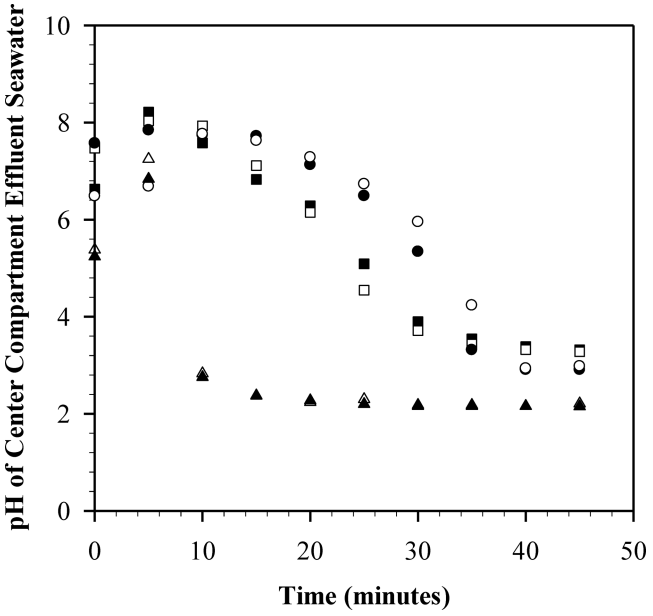

Figure 3. Average pH profiles for the four E-CEM configurations as a function of time at 20 A (408 A·m^{-2} current density): configuration 1, polarity A (●) and polarity B (○); configurations 2 and 3, polarity A (configuration 2) 50% cation-exchange resin with a capacity of 2.1 equiv·L^{-1} and 50% inert material (■) and polarity B (configuration 3) 100% cation-exchange resin with a capacity of 1 equiv·L^{-1} (□); configuration 4, polarity A (▲) and polarity B (△) at the same current density.

DOI: 10.1021/acs.energyfuels.6b02586
Energy Fuels 2017, 31, 1723−1730

for the pH to drop below 6 (bicarbonate and carbonate in the seawater re-equilibrate to CO_2 gas) for the average of two consecutive 45 min polarity cycles for each side of the module. Effluent seawater samples were collected every 5 min and their pHs measured. The initial pH of the influent Key West seawater was 8.04 ± 0.02.

In the second and third configurations the ion-exchange capacity was reduced in the electrode compartments from 2.1 to 1.0 equiv·L^{-1} using two different techniques. Side A of the module was filled with a mixture containing 50% cation-exchange resin with a capacity of 2.1 equiv·L^{-1} and 50% inert material. When side A (polarity A) is functioning as the anode, the module is operating as configuration 2. Side B of the module was filled with 100% cation-exchange resin with the capacity of 1 equiv·L^{-1}. When side B (polarity B) functions as the anode, the module is operating as configuration 3. The average of seven pH profiles for a given polarity shows that, for a defined current, both modifications reduce the effluent seawater equilibrium pH below 6 in approximately 20 min (Figure 3). A reduction in ion-exchange capacity from 2 to 1 equiv·L^{-1} allows the equilibrium conditions in the module after polarity switching to be re-established 26% faster in the second and third configurations of the module. When the polarity is reversed after a polarity cycle, the ion-exchange resin in the electrode compartment functioning as the anode is in the sodium Na^+ form, the H^+ ions generated at the anode exchange on the resin and the Na^+ ions released. The Na^+ ions then migrate through the cation-exchange membrane and into the center compartment. The migrating Na^+ ions pass through the cation-exchange membrane at the electrode now acting as the cathode and exchange on the resin to convert all the resin in that compartment to the sodium form. Equilibrium conditions are re-established during the polarity cycle when all the resin in the compartment now acting as the anode is regenerated back into the hydrogen form and all the resin in the cathode is regenerated back into the sodium form. This allows more H^+ ions to pass through the membrane closest to the anode to reduce the seawater pH below 6. The reduction in ion-exchange capacity enabled the resin to regenerate faster causing a 26% faster drop in seawater pH below 6 (Figure 3).

Commercial off the shelf CEDI end blocks were used to construct the first three E-CEM configurations. The data from the initial evaluation of these modules were used to custom design and build the fourth E-CEM. In this configuration the inert material is removed from the center compartment along with all the ion-exchange resin in the electrode compartments. The end blocks are placed in direct contact with the mesh electrodes, and the electrodes are positioned very close to the cation-exchange membranes (see Table 1). The average pH profiles of the consecutive polarity cycles in Figure 3 shows that by removing the electrically active ion-exchange material in the electrode compartments, equilibrium conditions are established within 7 min and the seawater pH drops below 6. In the first three configurations the initial H^+ ions produced at the anode were needed to regenerate the ion-exchange resin that was in the Na^+ form before excess H^+ could be used to lower the seawater pH. By designing and configuring the module without ion-exchange material, the initial H^+ ions produced at the anode are now used to lower the seawater pH instead of regenerating ion-exchange resin. This 65% improvement over configurations 2 and 3 in re-equilibration time is essential to achieving long-term feasibility of the process as switching the polarity of the module has become less energy intensive since CO_2 is recovered faster from the seawater.

Figure 4 compares the electrical resistance (voltage divided by amperage) profiles as a function of time for the four different

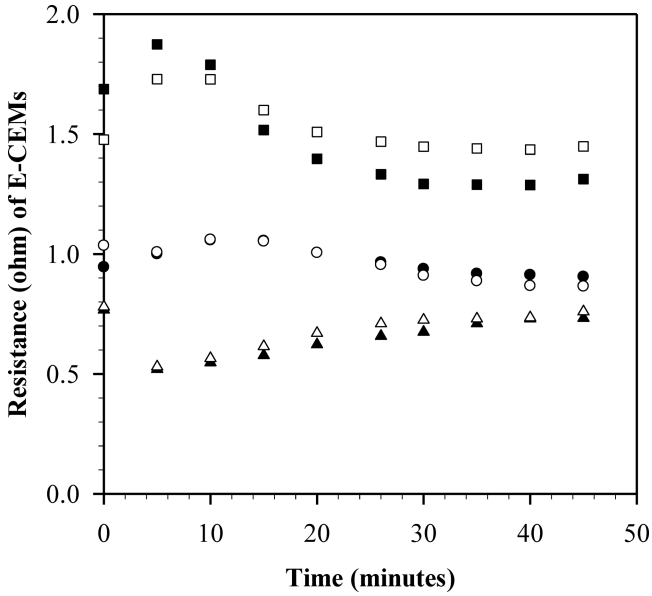

Figure 4. Average electrical resistance (Ω) profile comparisons for the four E-CEM configurations as a function of time, 45 min cycles at 20 A (408 A·m^{-2} current density): configuration 1, polarity A (●) and polarity B (○); configurations 2 and 3, polarity A (configuration 2) 50% cation-exchange resin with a capacity of 2.1 equiv·L^{-1} and 50% inert material (■) and polarity B (configuration 3) 100% cation-exchange resin with a capacity of 1 equiv·L^{-1} (□); and configuration 4, polarity A (▲) and polarity B (△).

module configurations at 20 A. The overpotential (~1.23 V) that is required for the evolution of the gases by water electrolysis (O_2 anode and H_2 cathode, Figure 1) at the electrodes was included in the calculation of resistance. Since the same operating conditions are maintained during the evaluations, the overpotential was the same in all module configurations. Including the overpotential has no impact on how the resistance values are used to compare the different configurations. The profiles indicate the modules containing 1 equiv·L^{-1} ion-exchange resin capacity in the electrode compartments had the highest electrical resistance over a 45 min polarity cycle. Of the two methods for reducing ion-exchange capacity in the electrode compartments, the configuration that reduced the resin capacity by adding 50% inert material to 50% resin at 2.1 equiv·L^{-1} appears to have the best electrical resistance performance. The electrical resistance performance on average over the 45 min polarity cycle is improved by as much as 35% in the configuration containing 100% resin at 2.1 equiv·L^{-1} capacity in the electrode compartments. However, this configuration takes 26% longer to re-equilibrate and seawater pH to drop below 6 after the polarity is switched at the end of a polarity cycle (Figure 3).

The difference in pH profiles and electrical resistance profiles for the first three module configurations can be explained by the conductivity of the individual components involved in ion transport within the modules. The conductivity (κ) in the modules is defined as the sum of five individual module components given in eq 13:

DOI: 10.1021/acs.energyfuels.6b02586
Energy Fuels 2017, 31, 1723−1730

$$\kappa = \kappa_1 + \kappa_2 + \kappa_3 + \kappa_4 + \kappa_5 \quad (13)$$

where κ_1 and κ_5 are the conductivities of the cation-exchange resin and reverse osmosis permeate mixture in the electrode compartments, κ_2 and κ_4 are the conductivities of the cation-exchange membranes, and κ_3 is the conductivity of the seawater and inert pellet mixture in the center compartment. κ_1 and κ_5 are dependent on the characteristics of the cation-exchange resin, particularly ion-exchange capacity and DVB (divinylbenzene) cross-linkage percentage. This will vary from one ionic form to another. κ_2 and κ_4 are fairly constant, while κ_3 is dependent on the ratio and particle size of the inert pellets. The electrical resistance, R (Ω), is related to the conductivity of the module by eq 14:

$$R = x/A\kappa \quad (14)$$

where x is the distance between the electrodes in cm and A is the electrode effective area in cm^2. The area A may be expressed as a function of the electrode length (y) and width (z) as given in eq 15 and provided as the effective electrode active area, 497 cm^2 (each) (Table 1).

$$A = (y)(z) \quad (15)$$

Figure 5 compares the average conductivity values for each module configuration. For the first three module configurations

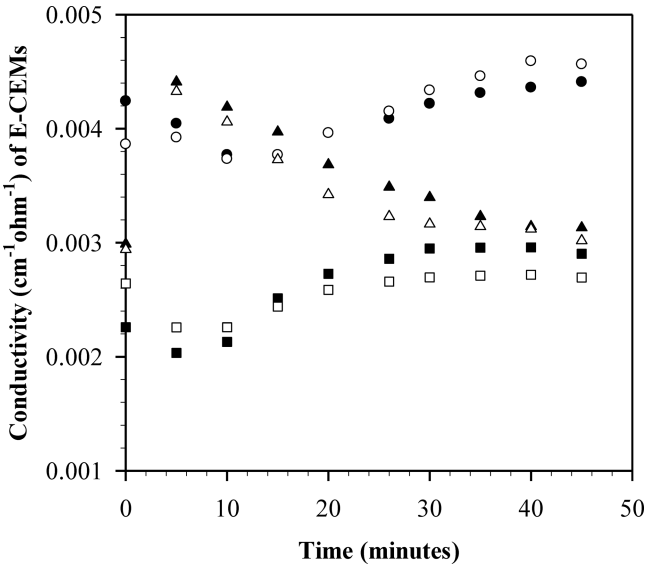

Figure 5. Average conductivity ($cm^{-1}\cdot\Omega^{-1}$) profile comparisons for the four E-CEM configurations as a function of time, 45 min cycles at 20 A (408 $A\cdot m^{-2}$ current density): configuration 1, polarity A (●) and polarity B (○); configurations 2 and 3, polarity A (configuration 2) 50% cation-exchange resin with a capacity of 2.1 equiv·L^{-1} and 50% inert material (■) and polarity B (configuration 3) 100% cation-exchange resin with a capacity of 1 equiv·L^{-1} (□); configuration 4, polarity A (▲) and polarity B (△).

constructed with commercial off the shelf end blocks, the conductivity is an average of 37% higher over the polarity cycle for the module containing 100% resin at 2.1 equiv·L^{-1} capacity in the electrode compartments. This form of the resin is more conductive than the configurations containing 1 equiv·L^{-1} capacity in the electrode compartments, and as a result less voltage to the module is needed to maintain the current over an average 45 min cycle. Less voltage results in less resistance within the module, and the average power requirements over a 45 min cycle measured 387 W. Figure 5 also suggests the configuration in which the resin capacity is reduced by adding 50% inert material to 50% resin at 2.1 equiv·L^{-1} is more conductive than the configuration containing 100% 1.0 equiv·L^{-1} resin capacity. The loss in conductivity results in an increase in module resistance and an increase in the average power requirements to 540−581 W. The significant loss in conductivity and increase in electrical resistance produced in the lower ion-exchange capacity module configurations minimizes any of the advantages gained by faster resin regeneration and lowering of the seawater pH obtained in these configurations (Figure 3). The results suggest that simply manipulating the ion-exchange resin inside a module assembled with commercial end blocks will not be enough to simultaneously (1) improve the re-equilibration time by increasing the ion transport properties between polarity cycles and (2) reduce the overall power requirements for the module by decreasing its resistance.

Since the ion-exchange material proved to be difficult to manipulate, the notion of its removal is attributed to electrolysis module configurations developed over the years for the treatment of brine and the regeneration of acid and base solutions.[20,21] To remove the ion-exchange material completely from the module, a new custom built module had to be designed such that the end blocks were placed in direct contact with the mesh electrodes. In this fourth configuration, the electrodes were positioned close to the ion-exchange membrane so that the H^+ ions produced at the anode would exchange across the membrane and not get swept away by the continuous flow of anolyte solution in the compartment. Table 1 shows how the electrode compartment volume and thickness in this new configuration were significantly reduced by placing the mesh electrode in contact with the ion-exchange membrane. This change in electrode volume and thickness also reduced the distance between the electrodes (x in eq 14). This new design relies solely on the conductivity of the ion-exchange membranes, anode, cathode, and seawater solutions.

Figure 4 shows how the electrical resistance profile for the fourth configuration initially decreases for the first 5 min and then slowly increases 29% over the course of the 45 min polarity cycle. More voltage is needed to maintain the current over an average 45 min cycle. This may be explained by the conductivity of the module. Figure 5 indicates that the conductivity of the module starts out better than the other three module configurations but deteriorates over the course of the 45 min polarity cycle. On average the fourth configuration is 15% less conductive than the first configuration and is 25% more conductive than configurations 2 and 3. While the average resistance over 45 min slowly increases by 29% over the polarity cycle, the electrical efficiency of the fourth configuration is 55% better than the second and third configurations of the module and 31% better than the first configuration of the module. As a result the average power consumption in configuration four is 265 W compared to configurations 1−3 (387, 540, and 581 W).

The custom design of the fourth module configuration effectively compensates for the removal of κ_1 and κ_5 variables that are dependent on the characteristics of the cation-exchange resin (eq 13). The 15% loss in conductivity in this module is compensated for by decreasing the distance between the electrodes from 1.94 to 1.14 cm as shown in eq 14 and Table 1. As a result the electrical resistance performance in this

DOI: 10.1021/acs.energyfuels.6b02586
Energy Fuels 2017, 31, 1723−1730

configuration is improved by 31% over the course of a polarity cycle and the power consumption is reduced.

CONCLUSIONS

Based on the evaluation of four E-CEM configurations significant progress has been made toward improving re-equilibration time in the module after switching the polarity and further improving the electrical efficiencies. The first three configurations proved to be the least efficient in energy consumption. However, the evaluation of these "proof of concept" configurations helped establish key variables responsible for ion transport in this application. As a result a fourth configuration was custom designed, built, and tested for this application. The custom module reached equilibrium upon polarity reversal 65% faster lowering seawater pH below 6 so that the carbonate and bicarbonate in the seawater are re-equilibrated to CO_2 gas for recovery. The electrical resistance of this module improved by 31%. These data will be used to further improve the design of the module for this specific application. The next variable to attempt to improve the energy efficiency is to increase the effective electrode active area as shown in eq 15. The ultimate goal is to successfully produce CO_2 and H_2 in quantities needed to make fuel at energy efficiencies similar to commercial electrolysis.

AUTHOR INFORMATION

Corresponding Author

*E-mail: Heather.Willauer@nrl.navy.mil.

ORCID

Heather D. Willauer: 0000-0002-2013-6859

Notes

The authors declare no competing financial interest.

[⊥]Emeritus.

ACKNOWLEDGMENTS

This work was supported by the Office of Naval Research both directly and through the Naval Research Laboratory. We acknowledge the NRL-Key West personnel for technical support.

REFERENCES

(1) Goeppert, A.; Czaun, M.; Surya Prakash, G. K.; Olah, G. A. Air as the renewable carbon source of the future: an overview of CO_2 capture from the atmosphere. *Energy Environ. Sci.* **2012**, *5*, 7833−7853.

(2) Markewitz, P.; Kuckshinrichs, W.; Leitner, W.; Linssen, J.; Zapp, P.; Bongartz, R.; Schreiber, A.; Müller, T. E. Worldwide innovations in the development of carbon capture technologies and the utilization of CO_2. *Energy Environ. Sci.* **2012**, *5*, 7281−7305.

(3) Huang, C.-H.; Tan, C.-S. A review CO_2 utilization. *Aerosol Air Qual. Res.* **2014**, *14*, 480−499.

(4) MacDowell, N.; Florin, N.; Buchard, A.; Hallett, J.; Galindo, A.; Jackson, G.; Adjiman, C. S.; Williams, C. K.; Shah, N.; Fennell, P. An overview of CO_2 capture technologies. *Energy Environ. Sci.* **2010**, *3*, 1645−1669.

(5) Peng, Y. P.; Yeh, Y. T.; Wang, P. Y.; Huang, C. P. A solar cell driven electrochemical process for the concurrent reduction of carbon dioxide and degradation of azo dye in dilute $KHCO_3$ electrolyte. *Sep. Purif. Technol.* **2013**, *117*, 3−11.

(6) Takahashi, T.; Broecker, W. S.; Bainbridge, A. E. The Alkalinity and Total Carbon Dioxide Concentration in the World Oceans. In *Carbon Cycle Modelling*; Bolin, B., Ed.; SCOPE: New York, 1981; Vol. *16*, pp 271−286.

(7) Takahashi, T.; Broecker, W. S.; Werner, S. R.; Bainbridge, A. E. Carbonate Chemistry of the Surface of the Waters of the World Oceans. In *Isotope Marine Chemistry*; Goldberg, E. D., Horibe, Y., Saruhashi, K., Eds.; Uchida Rokakuho: Tokyo, Japan, 1980; pp 291−326.

(8) Willauer, H. D.; DiMascio, F.; Hardy, D. R.; Lewis, M. K.; Williams, F. W. Development of an Electrochemical Acidification Cell for the Recovery of CO_2 and H_2 from Seawater. *Ind. Eng. Chem. Res.* **2011**, *50*, 9876−9882.

(9) Willauer, H. D.; DiMascio, F.; Hardy, D. R.; Lewis, M. K.; Williams, F. W. Development of an Electrochemical Acidification Cell for the Recovery of CO2 and H2 from Seawater II. Evaluation of the cell by Natural Seawater. *Ind. Eng. Chem. Res.* **2012**, *51*, 11254−11260.

(10) Willauer, H. D.; DiMascio, F.; Hardy, D. R.; Williams, F. W. Feasibility of CO_2 extraction from seawater and simultaneous hydrogen gas generation using a novel and robust electrolytic cation exchange module based on continuous electrodeionization technology. *Ind. Eng. Chem. Res.* **2014**, *53*, 12192−12200.

(11) Eisaman, M. D.; Parajuly, K.; Tuganov, A.; Eldershaw, C.; Chang, N.; Littau, K. A. CO2 Extraction from seawater using bipolar membrane electrodialysis. *Energy Environ. Sci.* **2012**, *5*, 7346−7352.

(12) Johnson, K. M.; King, A. E.; Sieburth, J. Coulometric TCO2 Analyses for Marine Studies: An Introduction. *Mar. Chem.* **1985**, *16*, 61.

(13) NEL Hydrogen, http://www.nel-hydrogen.com, accessed Jun. 18, 2015.

(14) Dermentzis, K. Continuous electrodeionization through electrostatic shielding. *Electrochim. Acta* **2008**, *53*, 2953−2962.

(15) Fedorenko, V. I. Ultrapure water production using continuous electrodeionization. *Pharm. Chem. J.* **2003**, *37*, 157−160.

(16) Lounis, A.; Setti, L.; Djennane, A.; Melikchi, R. Separation of Molybdenum-Uranium by a process combining ion exchange resin and membranes. *J. Appl. Sci.* **2007**, *7*, 1963−1967.

(17) Wood, J.; Gifford, J.; Arba, J.; Shaw, M. Production of ultrapure water by continuous electrodeionization. *Desalination* **2010**, *250*, 973−976.

(18) Keramati, N.; Moheb, A.; Ehsani, M. R. Effects of operating parameters on NaOH recovery from waste stream of Merox tower using membrane systems: Electrodialysis and electrodeionization processes. *Desalination* **2010**, *259*, 97−102.

(19) Kurup, A. S.; Ho, T.; Hestekin, J. A. Simulation and optimal design of electrodeionization process: Separation of multicomponent electrolyte solution. *Ind. Eng. Chem. Res.* **2009**, *48*, 9268−9277.

(20) Tzanetakis, N.; Taama, W. M.; Scott, K. Salt splitting in a three-compartment membrane electrolysis cell. *Filtr. Sep.* **2002**, *39*, 30−38.

(21) Coker, T. G.; LaConti, A. B.; Balko, E. N.; McGray, G. B. Electrolysis of alkali metal halides in a three compartment cell with self-pressurized buffer compartment. U.S. Pat.US 4,212,714, Jul. 15, 1980.

DOI: 10.1021/acs.energyfuels.6b02586
Energy Fuels 2017, 31, 1723−1730